OPEN

Citation: Cell Death and Disease (2013) 4, e669; doi:10.1038/cddis.2013.200

www.nature.com/cddis

Nicotinamide *N*-methyltransferase expression in SH-SY5Y neuroblastoma and N27 mesencephalic neurones induces changes in cell morphology via ephrin-B2 and Akt signalling

MG Thomas[1], M Saldanha[1], RJ Mistry[1], DT Dexter[2], DB Ramsden[3] and RB Parsons*[,1]

Nicotinamide *N*-methyltransferase (NNMT, E.C. 2.1.1.1) *N*-methylates nicotinamide to produce 1-methylnicotinamide (MeN). We have previously shown that NNMT expression protected against neurotoxin-mediated cell death by increasing Complex I (CxI) activity, resulting in increased ATP synthesis. This was mediated via protection of the NDUFS3 subunit of CxI from degradation by increased MeN production. In the present study, we have investigated the effects of NNMT expression on neurone morphology and differentiation. Expression of NNMT in SH-SY5Y human neuroblastoma and N27 rat mesencephalic dopaminergic neurones increased neurite branching, synaptophysin expression and dopamine accumulation and release. siRNA gene silencing of *ephrin B2* (EFNB2), and inhibition of Akt phosphorylation using LY294002, demonstrated that their sequential activation was responsible for the increases observed. Incubation of SH-SY5Y with increasing concentrations of MeN also increased neurite branching, suggesting that the effects of NNMT may be mediated by MeN. NNMT had no significant effect on the expression of phenotypic and post-mitotic markers, suggesting that NNMT is not involved in determining phenotypic fate or differentiation status. These results demonstrate that NNMT expression regulates neurone morphology *in vitro* via the sequential activation of the EFNB2 and Akt cellular signalling pathways.
Cell Death and Disease (2013) **4,** e669; doi:10.1038/cddis.2013.200; published online 13 June 2013
Subject Category: Neuroscience

Nicotinamide *N*-methyltransferase (NNMT, E.C. 2.1.1.1) catalyses the *N*-methylation of nicotinamide into 1-methylnicotinamide (MeN).[1] In the brain, NNMT expression is regionally distributed, occurring solely in neurones.[2] NNMT expression is elevated in numerous cancers, for example, bladder, lung and gastrointestinal tract,[3–5] and NNMT may serve as a prognostic marker for these cancers.[6,7] NNMT is hepatoprotective in hepatitis and cirrhosis[8] and protects against free radicals in pulmonary smooth muscle cells in chronic obstructive pulmonary disease.[9]

Using *post mortem* caudate nucleus and cerebella, we have shown that the expression of NNMT is increased in Parkinson's disease (PD) brains.[2,10] Stable expression of NNMT in the SH-SY5Y human neuroblastoma cell line, which has no endogenous expression of NNMT, at levels of activity comparable with that in PD brain, protected against the toxicity of the Complex I (CxI) inhibitors 1-methyl-4-phenylpyridinium ion and rotenone.[11] This protection was mediated via increased CxI activity and ATP production. Maintenance of CxI activity arose from protection of the 30 kDa subunit of CxI (NDUFS3) from degradation induced by 1-methyl-4-phenylpyridinium ion and rotenone. Thus increased NNMT expression may be a stress response of the neurone to the PD pathogenic process.

Induction of NNMT in renal clear cell carcinoma (RCC) cells activated matrix metalloproteinase-2, resulting in morphological changes as part of tumour metastasis.[12] Matrix metalloproteinase-2, which is involved in synaptic remodelling and synaptogenesis,[13] is upregulated by Akt signalling, which is activated by the expression of NNMT in RCC cells.[12] Akt, also known as protein kinase B, is a serine/threonine kinase that belongs to the cAMP-dependant protein kinase A/G/C superfamily and is at the centre of a myriad of cellular activities, including growth, proliferation, energy metabolism and migration.[14–16] The Akt pathway is activated by PI3 kinases, which phosphorylates Akt on residues Ser-473 and Thr-308, triggering downstream effects, including inhibition of p53, reduced expression of the pro-apoptotic gene Bim and increased translation of anti-apoptotic proteins.[14,16] Akt and phosphorylated Akt (Akt_{Pi}) are neuroprotective.[17–19]

[1]Institute of Pharmaceutical Science, King's College London, 150 Stamford Street, London SE1 9NH, UK; [2]Parkinson's Disease Research Group, Centre for Neuroinflammation and Neurodegeneration, Division of Brain Sciences, Imperial College London, Hammersmith Hospital, Du Cane Road, London W12 0NN, UK and [3]Department of Medicine, University of Birmingham, Edgbaston, Birmingham B15 2TH, UK
*Corresponding author: RB Parsons, Institute of Pharmaceutical Science, King's College London, 150 Stamford Street, London SE1 9NH, UK. Tel: +020 7848 4048; Fax: +020 7848 4800; E-mail: richard.parsons@kcl.ac.uk
Keywords: nicotinamide *N*-methyltransferase; cell signalling; phenotypic markers; neurone differentiation
Abbreviations: Akt_{Pi}, phosphorylated Akt; Akt_T, total Akt; ChAT, choline acetyltransferase; CxI, Complex I; DIC, differential interference contrast; EFNB2, ephrin B2; ephB, ephrin B receptor; MeN, 1-methylnicotinamide; NeuN, neuronal nuclei/FOX-3; NNMT, nicotinamide *N*-methyltransferase; PD, Parkinson's disease; RCC, renal clear cell carcinoma; TH, tyrosine hydroxylase
Received 27.3.13; revised 26.4.13; accepted 30.4.13; Edited by A Verkhratsky

Enhanced Akt expression is neuroprotective against the toxicity of 6-hydroxydopamine in PD models.[15,20] The abundance of Akt_{Pi} is significantly reduced in the dopaminergic neurones of the substantia nigra in PD patients,[21] and the neuroprotective effects of rasagiline are mediated via the activation of Akt signalling.[22]

Akt phosphorylation is activated by the ephrin B receptor (ephB),[20,23] whose ligand ephrin B2 (EFNB2) is induced alongside NNMT as a result of increased hedgehog signalling in pancreatic cancer cells.[24] EFNB2 regulates transcellular communication via interaction with ephB3 and B4 receptors, tyrosine kinases present on the post-synaptic termini of adjacent target cells.[25] In the brain, EFNB2/ephB receptor signalling is involved in regulating neuronal and axonal migration, synaptic formation, function and plasticity[26–29] via interaction with a number of pre- and post-synaptic targets.[30] Activation of the phosphorylation of Akt by the ephB receptor gives rise to morphological and functional changes such as increased synaptic formation, regulation of neuronal plasticity[29] and protection of SH-SY5Y cells against the toxicity of 6-hydroxydopamine.[20]

From the above, it can be seen that increased NNMT expression is a feature of rapidly dividing cancer cells and in neurones as a response to stressful states, such as PD. Therefore, we explored the effect of NNMT expression upon neuronal morphology and differentiation using our SH-SY5Y cell model of NNMT expression (S.NNMT.LP).[11] In addition, we have used a second cell line, N27–rat mesencephalic dopaminergic neurones–to confirm our findings.

Results

NNMT expression increased neurite branching and the presynaptic marker synaptophysin. To investigate the effect of NNMT expression upon neurone morphology, we used the S.NNMT.LP cell line, produced as part of our ongoing studies by the stable transfection of SH-SY5Y with a plasmid encoding NNMT C-terminally fused to the V5 epitope.[11] A single *NNMT* mRNA transcript and a single NNMT-V5 protein of the correct molecular weight were expressed solely in S.NNMT.LP cells (Supplementary Figures S1A and S1B). Cell death was significantly lower in S.NNMT.LP compared with SH-SY5Y cells (Supplementary Figure S1C).

NNMT expression has been shown to induce morphological changes in RCC cells, so we hypothesised that NNMT-V5 expression may have a similar effect upon SH-SY5Y morphology. Changes in SH-SY5Y morphology were determined using phase contrast and differential interference contrast (DIC) microscopy. DIC imaging allowed easier analysis of neurite branches compared with phase-contrast images. Under phase-contrast microscopy, SH-SY5Y cells appeared rounded and showed a basic neuronal morphology (Supplementary Figure S2, top panels), with a limited number of neurites, intercellular connections and neurite branching. By contrast, S.NNMT.LP cells appeared more elongated (Supplementary Figure S2B, bottom panels), with increases in the number of neurites per cell and the degree of branching. The number of intercellular connections also increased.

Quantification using image analysis demonstrated that neurite length was lower in S.NNMT.LP compared with that of SH-SY5Y cells (18% decrease, $P=0.0288$; Figures 1a and b). The number of neurites per cell was increased in S.NNMT.LP compared with the number in SH-SY5Y cells (11% increase, $P<0.001$; Figure 1b top right panel), and the number of branches per neurite of S.NNMT.LP was significantly higher than those of SH-SY5Y cells (71% increase, $P=0.0164$) (Figure 1b bottom left panel). In SH-SY5Y cells, 39.6% of neurites had no branching (Figure 1b bottom right panel), 28.7% had 1 branch, 20.8% had either 2 or 3 branches, and only 10.9% of neurites had ≥ 4 branches. By contrast, in S.NNMT.LP cells, only 19.2% of neurites had no branches, 19.7% had only one branch 41.5% had either 2 or 3 branches; and a further 19.6% of neurites had ≥ 4 branches. Thus neurite branching was increased significantly in S.NNMT.LP cells compared with the parental SH-SY5Y cells.

We next investigated whether S.NNMT.LP demonstrated an increase in the expression of the presynaptic marker synaptophysin.[31] Synaptophysin expression was detected as a 38 kDa protein in both SH-SY5Y and S.NNMT.LP cell lines (Figure 1c left panel). Expression of synaptophysin was significantly increased in S.NNMT.LP compared with that seen in SH-SY5Y cells (Figure 1c right panel, 41.4% increase, $P=0.004$, $n=4$).

The effect of NNMT upon neurone morphology was also investigated using N27 cells. Substantia nigra dopaminergic neurones are derived from the mesencephalon,[32] hence N27 cells closely mimic dopaminergic neurones of the substantia nigra. Wild-type N27 cells expressed no *NNMT* mRNA (Supplementary Figure S3). Transient transfection of N27 using the pNNMT.D plasmid[11] resulted in robust NNMT-V5 expression (Figure 1d left panel). Synaptophysin expression was undetectable in mock-transfected N27 cells, whereas transient expression of NNMT-V5 resulted in robust synaptophysin expression. Mock-transfected N27 cells demonstrated a degree of neuronal morphology but with very few neurites and no interneuronal connections (Figure 1d right panel). N27 cells expressing recombinant NNMT-V5 had significantly more neuronal processes with the presence of a number of interneuronal connections (Figure 1d right panel). These results confirm that NNMT-V5 expression induced the formation of neurites and the expression of synaptophysin in dopaminergic mesencephalic neurones.

NNMT expression increased dopamine uptake and release. Next, we investigated whether dopamine uptake and release was increased by NNMT-V5 expression. Dopamine accumulation was significantly increased in S.NNMT.LP compared with SH-SY5Y cells (Figure 1e left panel, 4.8-fold increase, $P=0.0154$), with a corresponding increase in dopamine release (Figure 1e middle panel, 7.3-fold increase, $P=0.0182$). The percentage of the dopamine pool released was not significantly different in S.NNMT.LP compared with SH-SY5Y cells (Figure 1e right panel). Taken together, these results show that NNMT-V5 expression in SH-SY5Y cells changed cellular morphology and increased dopamine uptake and release.

The effects of NNMT expression were mediated via activation of EFNB2/Akt signalling. The next step was to elucidate the signalling pathway involved using S.NNMT.LP

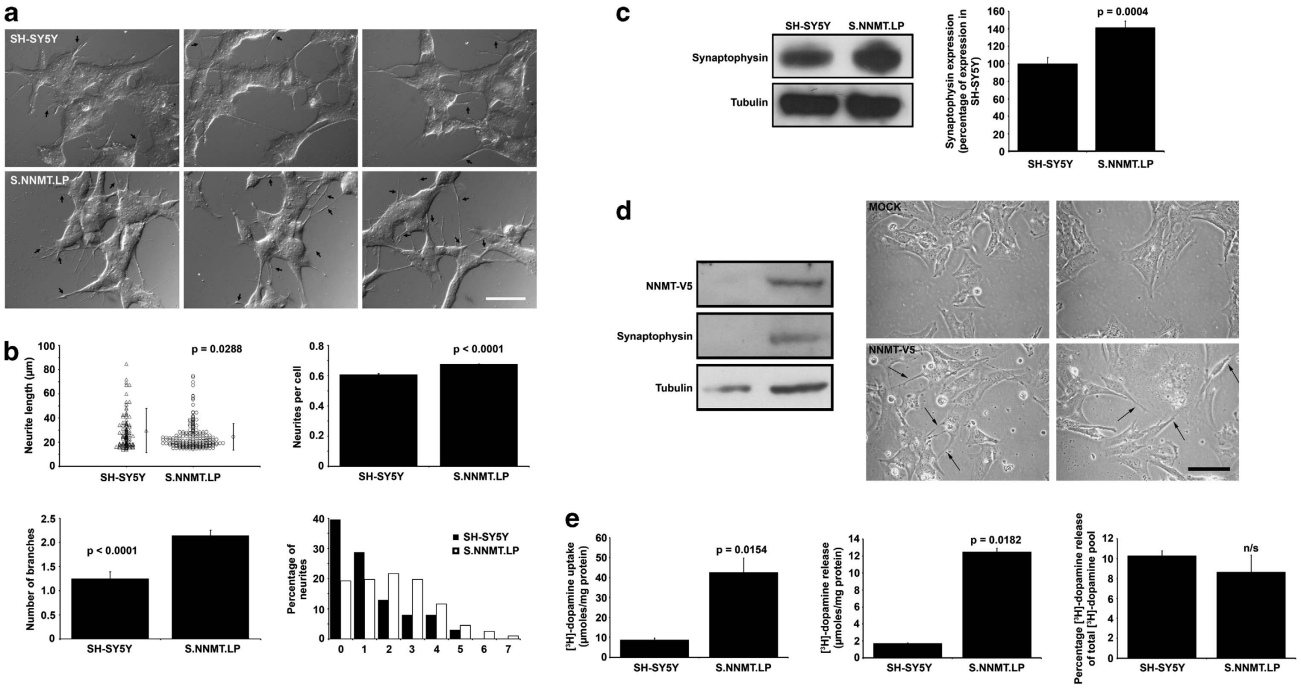

Figure 1 Expression of NNMT-V5 increased neurite branching and increased both synaptophysin expression and dopamine uptake and release. (**a**) DIC microscopic images of SH-SY5Y and S.NNMT.LP. Neurites of S.NNMT.LP cells appeared to have more branches than SH-SY5Y neurites. Arrows indicate points of neurite branching. Bar = 50 μm. (**b**) Quantitative image analysis of DIC microscopic images. Average neurite length was significantly lower in S.NNMT.LP cells compared with SH-SY5Y. The number of neurites per cell and the number of neurite branches was significantly higher in S.NNMT.LP cells. The distribution of branches per neurite was shifted towards neurites having more branches in S.NNMT.LP cells. Error bars represent S.E.M. (**c**) Quantitative western blot analysis of synaptophysin expression in SH-SY5Y and S.NNMT.LP cells. Synaptophysin expression was significantly increased in S.NNMT.LP cells. Error bars represent S.D. (**d**) Effect of transient expression of NNMT-V5 in N27 cells upon synaptophysin expression and neuronal morphology. Both NNMT-V5 and synaptophysin were detected only in N27 cells transiently transfected with pNNMT-V5. NNMT-V5-expressing N27 cells demonstrated neurites (arrowed), which were absent in mock-transfected N27 cells. Bar = 50 μm. (**e**) Dopamine accumulation and release in SH-SY5Y and S.NNMT.LP cells. Dopamine accumulation (left) and K^+-evoked dopamine release (middle) were significantly increased in S.NNMT.LP cells. The proportion of the dopamine pool released upon K^+ stimulation (right panel) did not alter upon NNMT expression. Error bars represent S.D. NS = not significant

cells. The first candidate investigated was the EFNB2 signalling pathway. Both SH-SY5Y and S.NNMT.LP cell lines expressed a single *EFNB2* mRNA transcript. EFNB2 protein expression was detected as two bands of approximately 49 and 28 kDa (Figure 2a upper panel), corresponding to the full-length and ectodomains of EFNB2, respectively.[33,34] *EFNB2* mRNA expression was significantly increased in S.NNMT.LP compared with that in SH-SY5Y cells (189% increase, $P = 0.0037$, $n = 4$). Levels of both 49 and 28 kDa immunoreactive proteins was significantly higher in S.NNMT.LP cells (Figure 2a bottom panel, 564% increase, $P = 0.0014$ for 48 kDa protein, 612% increase, $P = 0.0182$ for 28 kDa protein, $n = 3$ for both).

We investigated whether there was increased Akt phosphorylation, as Akt is a downstream target of EFNB2. Both total Akt (Akt_T) and Akt_{Pi} were detected as a single band of approximately 60 kDa in both SH-SY5Y and S.NNMT.LP cells, demonstrating robust expression of both (Figure 2b upper panel). Akt_T expression was not significantly different in S.NNMT.LP cells compared with that observed in SH-SY5Y (Figure 2b lower panel, 4.2% decrease, $P = 0.5179$, $n = 3$), whereas Akt_{Pi} was increased in the presence of NNMT-V5 (35% increase, $P = 0.0044$, $n = 3$). Accordingly, the Akt_{Pi}:Akt_T ratio increased in response to NNMT-V5 expression (41.3% increase, $P = 0.0248$, $n = 3$).

Next we demonstrated that EFNB2 was responsible for the increase in Akt_{Pi} and synaptophysin expression we observed in S.NNMT.LP cells (Figure 3a). Silencing of *EFNB2* expression in S.NNMT.LP cells (S.NNMT.LP^{EFNB2-}) resulted in a significant decrease in EFNB2 compared with S.NNMT.LP cells transfected with scrambled siRNA (S.NNMT.LP^{WT}; data not shown). Silencing of EFNB2 expression resulted in a significant decrease in Akt_{Pi} (81.9% decrease, $P = 0.0004$, $n = 4$) and the Akt_{Pi}:Akt_T ratio (77.7% decrease, $P < 0.0001$, $n = 4$), with no effect upon Akt_T (18.9% decrease, $P = 0.06$, $n = 4$). Silencing of EFNB2 expression significantly reduced synaptophysin expression (46.1%, $P = 0.0006$, $n = 4$). Silencing of EFNB2 expression resulted in a small yet significant reduction in the number of neurites per S.NNMT.LP^{EFNB2-} cell compared with that in S.NNMT.LP^{WT} (0.79 ± 0.067 *versus* 0.7 ± 0.06, 11% reduction, $P < 0.0001$) (Figure 3b). Quantitative analysis of neurite length demonstrated that average neurite length in S.NNMT.LP^{EFNB2-} cells was increased compared with that of S.NNMT.LP^{WT} cells (35% increase, $P = 0.0005$), with many neurites being hyper-elongated in S.NNMT.LP^{EFNB2-} cells.

Finally, we investigated whether the phosphorylation of Akt was responsible for increased synaptophysin expression. Incubation of S.NNMT.LP cells with 50 μM LY294002 decreased Akt_{Pi} (50% decrease, $P = 0.0034$, $n = 4$), the

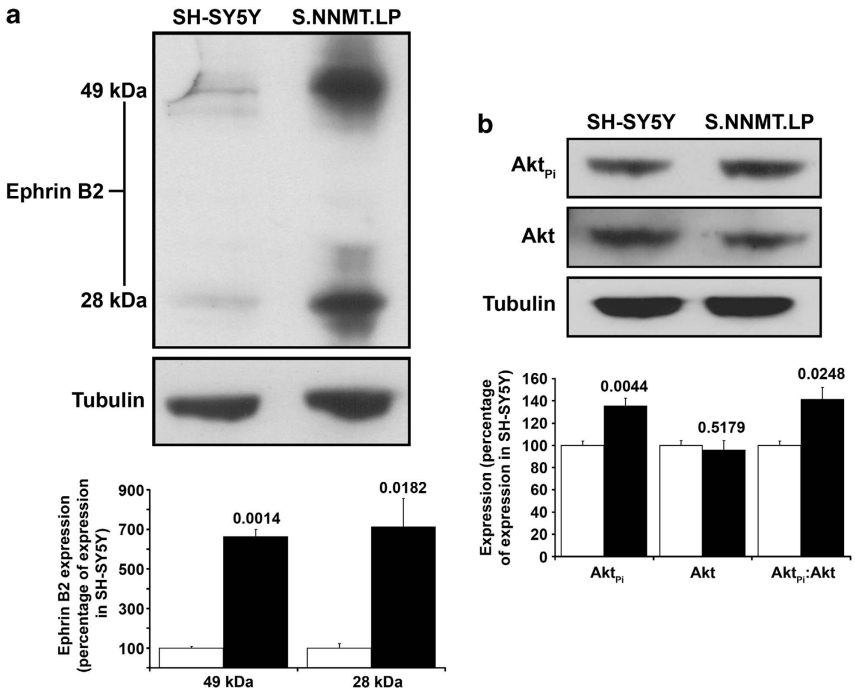

Figure 2 NNMT-V5 expression activated the EFNB2/Akt cell signalling pathway. (**a**) Quantitative western blot analysis of EFNB2 expression in SH-SY5Y and S.NNMT.LP cells. EFNB2 was detected as two bands of 49 and 28 kDa, corresponding to the full-length and cleaved forms, respectively. The expression levels of both were significantly increased in S.NNMT.LP. (**b**) Quantitative analysis of Akt_T and Akt_{Pi} expression in SH-SY5Y and S.NNMT.LP cells. The expression of Akt_{Pi} and the Akt_{Pi}:Akt_T ratio were significantly increased in S.NNMT.LP, whereas the expression of Akt_T was unchanged. Error bars represent S.D. For both the panels, white bars = SH-SY5Y, black bars = S.NNMT.LP

Akt_{Pi}:Akt_T ratio (46.3% decrease, $P=0.0052$, $n=4$) and synaptophysin expression (56.3% decrease, $P=0.001$, $n=4$) (Figure 3c). These results demonstrate that the effects of NNMT-V5 expression upon SH-SY5Y cells were mediated via the sequential activation of the EFNB2 and Akt signalling pathways.

MeN replicated the effects of NNMT expression upon SH-SY5Y neurite branching. We next determined whether MeN, the metabolic product of NNMT, replicated the effects of NNMT-V5 upon SH-SY5Y morphology using DIC microscopy (Figure 4a). The amount of neurite branching appeared to be higher in SH-SY5Y cells incubated with MeN compared with untreated cells. The length of neuritic processes did not significantly increase with increasing MeN concentration (Figure 4b top left panel, $26.6 \pm 14.7\,\mu$m in untreated cells, compared with 30.1 ± 20.6, 30.7 ± 18.7 and $31.4 \pm 17.7\,\mu$m for 0.25, 0.5 and 1 mM MeN, respectively). The number of neuritic processes per cell incubated in 1 mM MeN increased by 10% compared with untreated cells (Figure 4b top right panel, 0.834 ± 0.002 *versus* 0.918 ± 0.016, $P<0.001$). The degree of neurite branching increased significantly in the presence of all concentrations of MeN (Figure 4b bottom left panel). In untreated cells, there were an average of 1.3 ± 0.1 branches per neurite, which increased to 2.9 ± 0.2 in cells incubated with 1 mM MeN, an increase of 124% ($P<0.001$). In all, 39% of neurite processes had no branching, with a further 26% only having one branch; only 5% of neurite processes had ≥ 4 branches (Figure 4b bottom right panel). This distribution shifted with increasing MeN concentration, with 19% of neuritic processes having ≥ 4 branches in cells cultured in the presence of both 0.25 mM and 0.5 mM MeN and 33% of neuritic processes having ≥ 4 branches in cells incubated in the presence of 1 mM MeN.

NNMT reduced cholinergic phenotype but did not induce terminal differentiation. In light of the increased dopamine uptake and release induced by NNMT-V5 expression, we investigated whether NNMT-V5 expression was involved in SH-SY5Y differentiation using western blotting analysis of various pan- and cell-specific neuronal markers using mouse brain homogenate as a positive control (Figure 5). The cholinergic marker Choline acetyltransferase (ChAT) was expressed as a $\sim$70 kDa protein in both SH-SY5Y and S.NNMT.LP cells and as a $\sim$72 kDa protein in mouse brain, which is in accord with published reports.[35,36] ChAT expression was significantly lower in S.NNMT.LP cells (66% reduction, $P=0.0066$, $n=4$). The serotonergic marker tryptophan hydroxylase was expressed in SH-SY5Y, S.NNMT.LP and mouse brain as a $\sim$56 kDa protein and was unchanged by the expression of NNMT-V5 (7.1% decrease, $P=0.3515$, $n=4$). The dopaminergic/noradrenergic marker tyrosine hydroxylase (TH) was expressed in mouse brain as a $\sim$56 kDa protein and was undetected in both SH-SY5Y and S.NNMT.LP cells. The post-mitotic marker neuronal nuclei/FOX-3 (NeuN) was expressed in SH-SY5Y, S.NNMT.LP and mouse brain as a double band of $\sim$40–45 kDa protein as previously described.[37] NeuN expression was unchanged by the expression of NNMT-V5

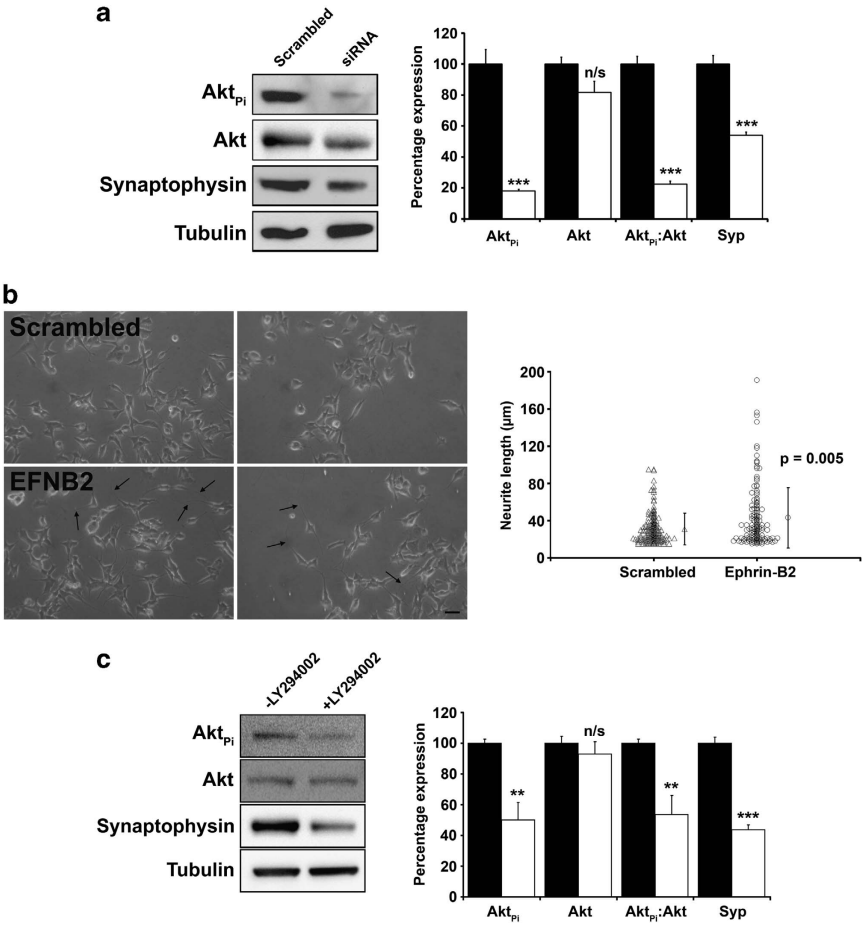

Figure 3 The sequential activation of the EFNB2 and Akt signalling pathways mediated the effects of NNMT-V5 expression in S.NNMT.LP cells. (**a**) Quantitative western blotting analysis of the effect of *EFNB2* gene silencing upon Akt_{Pi}, Akt_T and synaptophysin expression. esiRNA silencing of *EFNB2* expression significantly reduced Akt_{Pi}, Akt_{Pi}:Akt_T and synaptophysin protein expression and had no effect upon Akt_T expression. Error bars represent S.D. (**b**) Quantitative image analysis of S.NNMT.LP cells. esiRNA silencing of *EFNB2* expression significantly altered neurite morphology (highlighted by arrows). Average neurite length was significantly higher in S.NNMT.LP cells in which *EFNB2* expression had been silenced. Error bars represent S.E.M. Bar = 50 μm. (**c**) Quantitative western blotting analysis of the effect of the Akt phosphorylation inhibitor LY294002 upon Akt_{Pi}, Akt_T and synaptophysin expression. Incubation of S.NNMT.LP with LY294002 significantly reduced Akt_{Pi} and synaptophysin expression and had no effect upon Akt_T expression. Error bars represent S.D. For all panels, $^{**}P<0.01$, $^{***}P<0.001$, NS = not significant, black bars = SH-SY5Y, white bars = S.NNMT.LP, Syp = synaptophysin

(12.9% decrease, $P=0.2934$, $n=4$). Therefore, NNMT expression reduced cholinergic phenotype but did not induce dopaminergic/noradrenergic, serotonergic or terminal differentiation.

Discussion

In this study, we show that NNMT expression increased the number of neurites per cell, the number of branches per neurite, the expression of the presynaptic marker synaptophysin and the uptake and release of dopamine in SH-SY5Y stably expressing NNMT-V5 (S.NNMT.LP). The effects upon neurite formation and synaptophysin expression were also repeated in N27 cells transiently expressing NNMT-V5. These changes were shown to be brought about via the induction of the EFNB2 and Akt cell signalling pathways, in that the expression of NNMT was shown to activate these pathways, whereas blockage of the pathways using (1) siRNA gene silencing of *EFNB2* and (2) inhibition of Akt phosphorylation using LY294002 abolished the effects of NNMT-V5 expression. We also showed that the effects of NNMT-V5 expression upon neurite branching were replicated by the addition of MeN.

Although SH-SY5Y cells are widely used in neurodegenerative disease research, their suitability for such studies is controversial.[38] SH-SY5Y are a tumour-derived pan-neuronal cell line maintained in continuous culture, which require terminal differentiation in order to phenotypically and morphologically resemble true neurones. Using various differentiation protocols, a number of neuronal phenotypes can be produced.[39–41] Although a tumour-derived cell line, it is apparent from their robust expression of synaptophysin and ability to accumulate and release dopamine that undifferentiated SH-SY5Y cells do possess neuronal characteristics, which make them useful for studies such as ours. SH-SY5Y cells do not express NNMT, a fact we exploited in studies on the effects of NNMT expression.[11] Thus, the combination of SH-SY5Y and S.NNMT.LP cells is an ideal model for investigating the molecular pathways underlying the cellular effects of NNMT. We also confirmed key experimental results

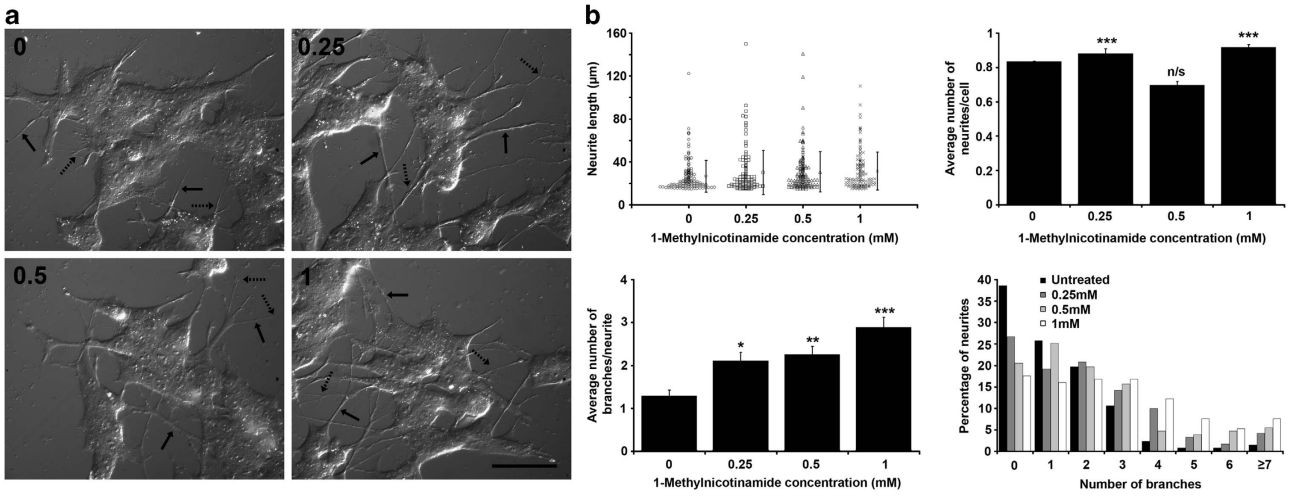

Figure 4 Incubation of SH-SY5Y with MeN increased neurite branching. (**a**) DIC microscopic images. Increasing concentrations of MeN appeared to increase the number of neurite branches (arrows). Numbers in images represent concentration of MeN. Bar = 50 μm. (**b**) Quantitative image analysis. Increasing concentrations of MeN had no significant effect upon neurite length. By contrast, the the average number of neurites per cell and the number of neurite branches increased with increasing concentration of MeN. Analysis of the population distribution of neurite branching showed that there was an increase in the number of neurite branches with increasing MeN concentration. Error bars represent S.E.M. $^{*}P<0.05$, $^{**}P<0.01$, $^{***}P<0.001$, NS = not significant

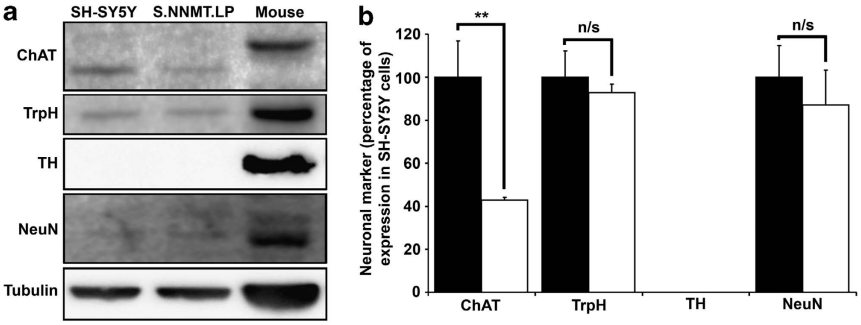

Figure 5 NNMT-V5 expression decreased ChAT expression but had no effect upon final phenotype nor terminal differentiation. (**a**) Western blotting analysis of neuronal markers. The phenotypic markers ChAT (cholinergic) and tryptophan hydroxylase (TrpH; serotonergic), along with the post-mitotic marker NeuN, were all detected as either single bands (phenotypic markers) or as a double band (NeuN), whereas by contrast the dopaminergic marker TH was not detected in either SH-SY5Y or S.NNMT.LP cells. (**b**) Quantitative densitometric analysis. The expression level of ChAT was significantly reduced in S.NNMT.LP, whereas that of TrpH, TH and NeuN were unaltered. Error bars represent S.D. $^{**}P<0.01$, NS = not significant

(changes in cellular morphology and synaptophysin expression) using N27 cells, an immortalised rat mesencephalic neuronal cell line which expresses TH.[42] Although also a cell line maintained in continuous culture, N27 were produced by the immortalisation of dopaminergic neurones derived from embryonic day 12 rat mesencephalon using the SV40 large T antigen.[43,44] Such a paradigm allows us to negate the possibility that the morphological effects observed arose as a consequence of the tumourigenic nature of SH-SY5Y cells.

The most significant result of our study is that, in both SH-SY5Y and N27 cells, expression of NNMT induced changes in morphology via the sequential activation of the EFNB2 and Akt signalling pathways. NNMT did not induce terminal differentiation as evidenced by the lack of change in the expression of the post-mitotic marker NeuN and the continued replication of both S.NNMT.LP and transiently transfected N27 cells. Also, NNMT does not appear to have a major role in determining dopaminergic phenotypic fate, demonstrated by both the lack of change in TH expression and the dopaminergic phenotype of N27 cells, which do not express NNMT. The activation of the EFNB2 and Akt signalling pathways has been shown to induce morphological changes, such as neuronal and axonal migration;[27,29] thus the ability of NNMT to activate EFNB2 and Akt signalling elevates NNMT from historically being considered to be a component of Phase II metabolism to regulating fundamental cell signalling pathways involved in neuronal development and survival.

It should be noted that, due to the pan-neuronal nature of the cell lines used, the effects that we observe in this study may not be replicated in terminally differentiated, non-dividing neurones *in vivo*. However, if these results were to be replicated, they would provide further evidence that the increased NNMT expression that we have observed in PD patients[2,10] may not be part of the pathogenic process but instead may be a stress response. However, enhanced NNMT expression may be toxic *in vivo* in a manner that cannot be observed using our *in vitro* models. A small number of studies have suggested that MeN is toxic towards

neurones, using supraphysiological concentrations of MeN,[45–47] which are unlikely to be achieved even under conditions of high NNMT expression. It is also possible that NNMT may deleteriously affect pyridine nucleotide production, but although we have previously shown that NNMT expression reduced pyridine nucleotide synthesis, this had no deleterious effect upon SH-SY5Y cell survival.[11] Finally, NNMT may potentially increase the production of methylated tetrahydroisoquinolines and β-carbolines, endogenously produced compounds which inhibit CxI;[48] however, as yet there is no direct experimental evidence that NNMT is responsible for the production of such compounds.

Materials and Methods

Unless otherwise stated, all materials were obtained from Sigma-Aldrich (Poole, Dorset, UK) and were of the highest purity available. Male C57BL/6 mice were obtained from the Biological Services Unit, King's College London, London, UK from which brain homogenate was prepared as previously described.[2]

Cell culture incubations. SH-SY5Y human neuroblastoma and S.NNMT.LP cells (SH-SY5Y stably expressing NNMT produced as part of our ongoing studies) were cultured as previously described.[11] Recombinant NNMT (NNMT-V5) expression and reduced S.NNMT.LP cell death compared with SH-SY5Y were confirmed as previously described.[11] For all experiments, SH-SY5Y cells at passage 19–22 and S.NNMT.LP cells at passage number 7–9 (which correlates approximately with passage 22–24 for SH-SY5Y) were used. In order to facilitate the investigation of the effect of NNMT upon cell morphology and differentiation, both SH-SY5Y and S.NNMT.LP cells were used in their undifferentiated state. N27 rat mesencephalic dopaminergic neurones were cultured in AQMedia (Sigma, Poole, UK) supplemented with 10% FBS, 2 mM glutamine and 100 U/ml penicillin/streptomycin.

Cell morphology analysis. SH-SY5Y and S.NNMT.LP cell morphology was quantitatively analysed by DIC microscopy at 37 °C using a Zeiss AxioPlan 2 microscope (Carl Zeiss, Welwyn Garden City, UK) with a $\times 40$ objective lens, combined with image analysis involving three measures of cellular morphology: neurites per cell, neurite length, and the number of neurite branches. SH-SY5Y and S.NNMT.LP cells were incubated on poly-*L*-lysine-coated glass microscopy slides overnight, after which they were mounted in media under a coverslip. Image analysis was performed using Adobe Photoshop CS2 (Adobe Systems, San Jose, CA, USA) on seven independent images for each cell line. The total number of cells counted was 184 for SH-SY5Y and 294 for S.NNMT.LP. Only neurites $>15\,\mu$m in length were considered as true neuritic processes and as such counted. The number of neuritic processes per image was counted, normalised for the number of nuclei present in the image and expressed as neuritic processes per cell ± S.E.M. The total number of neuritic processes counted was 132 for SH-SY5Y and 198 for S.NNMT.LP. The lengths of these neurites were measured and expressed as the average neuritic process length in μm ± S.E.M. The number of branches of each neurite included in the above analyses was counted and expressed as number of branches per neurite ± S.E.M. The population distribution of the number of neurite branches per neurite was also calculated and expressed as a percentage of neurites.

The effect of MeN upon SH-SY5Y cell morphology was also quantitatively assessed using DIC. Cells were incubated as above for 24 h in media supplemented with 0, 0.25, 0.5 and 1 mM MeN. Five unique images were analysed for each incubation condition with the following total number of cells per incubation condition counted: 184 (untreated), 143 (0.25 mM MeN), 183 (0.5 mM MeN), and 146 (1 mM MeN). The total number of neuritic processes counted per incubation condition were 132 (untreated), 120 (0.25 mM MeN), 127 (0.5 mM MeN), and 131 (1 mM MeN).

Transient expression of NNMT in N27 cells. N27 cells were seeded at a density of 75 000 cells/ml into the wells of a six-well plate and allowed to grow until approximately 75% confluent. Cells were transiently transfected using the pNNMT-D plasmid, which encodes NNMT C-terminally fused with the V5 epitope.[11] After 48 h, recombinant NNMT-V5 expression was detected using western blotting. Cells were imaged under phase-contrast microscopy using a Canon D30 digital SLR camera mounted to an Axiovert C40 microscope (Zeiss).

[^{3}H]-Dopamine accumulation and release. The uptake and subsequent accumulation of [^{3}H]-dopamine by SH-SY5Y and S.NNMT.LP cells were measured using the method of Lam *et al.*[49] Specific dopamine uptake by dopamine transporters was differentiated from non-specific dopamine uptake by incubating identical samples in Krebs–Hepes buffer supplemented with 10 μM nomifensine.[50] After accumulation, the cells were washed thrice with Krebs/HEPES for 15 min each and placed directly in ice. Cells were lysed using phosphate-buffered saline supplemented with 1% (v/v) Triton X-100 for 20 min, after which the homogenate was transferred into microcentrifuge tubes and centrifuged briefly to remove particulate material. [^{3}H]-Dopamine was measured in the samples by mixing the homogenate 1 : 3 with Ultima Gold XR scintillation cocktail and counted using scintillation spectroscopy (Beckman, High Wycombe, UK). Further samples were assayed for protein concentration, and [^{3}H]-dopamine accumulation was calculated and expressed as nmoles dopamine/mg protein/min ± S.D.

Dopamine release from cells was stimulated using 50 mM potassium as previously described.[51] After stimulation for 5 min, the cells were placed immediately in ice. The stimulation buffer was transferred without delay into microcentrifuge tubes and centrifuged briefly to pellet any particulate material and [^{3}H]-dopamine counts were measured as described above. Further samples were assayed for protein concentration and stimulated [^{3}H]-dopamine release was calculated and expressed as nmoles dopamine released/mg protein/min ± S.D. Additionally, the fraction of the total dopamine pool released was calculated and expressed as a percentage of total dopamine pool released ± S.D.

Reverse transcriptase PCR detection of NNMT expression. mRNA was isolated from SH-SY5Y and N27 cells and expression of *NNMT* mRNA was assessed using RT-PCR as described previously.[11]

Quantitative PCR analysis of EFNB2 mRNA expression. The expression of *EFNB2* mRNA was quantified in SH-SY5Y and S.NNMT.LP cells using real-time quantitative PCR as previously described,[11] using mRNA primers and the appropriate Universal Probe Library probes as internal quantification probe (Roche, Burgess Hill, UK) as outlined in Table 1. The housekeeping genes *β-actin* and *glyceraldehyde-3-phosphate dehydrogenase* (Table 1) were used to normalise mRNA expression. Results were calculated using the $\Delta\Delta$Ct method and expressed as a percentage of expression compared with SH-SY5Y cells ± S.D., with *EFNB2* mRNA in SH-SY5Y cells assigned an expression level of 100%. The presence of single bands in each sample was subsequently confirmed using DNA gel electrophoresis.

Quantitative western blot analysis of protein expression. The expression levels of recombinant NNMT (NNMT-V5), EFNB2, synaptophysin, Akt_T protein, TH, tryptophan hydroxylase, ChAT, NeuN and Akt_{Pi} were quantified using quantitative western blotting.[11] Proteins were detected as outlined in Table 2, and proteins were visualised using electrochemiluminescent detection. To normalise for protein concentration, membranes were stripped using Restore Western Stripping Reagent (Fisher Scientific, Loughborough, UK) and reprobed for β-tubulin as outlined in Table 2. Images were digitally captured, band intensities were quantified using densitometric analysis using the GeneTools image analysis software (Syngene, Cambridge, UK) and normalised for β-tubulin expression. Protein expression was calculated and expressed as a percentage of the intensity observed in control cells ± S.D. Synaptophysin and NNMT-V5 expression levels in N27 cells were not quantified. Additionally, Akt phosphorylation was calculated by dividing the Akt_{Pi} by the Akt_T intensity to produce the Akt_{Pi}:Akt_T ratio, which was subsequently expressed as a percentage of Akt_{Pi}:Akt_T observed in control cells ± S.D.

siRNA-mediated silencing of EFNB2 expression. *EFNB2* expression was silenced in S.NNMT.LP using MISSION *EFNB2* esiRNA (Invitrogen, Paisley, UK). S.NNMT.LP cells were plated at a density of 75 000 cells/ml into the wells of a six-well plate and allowed to settle overnight, at which point cells were approximately 50% confluent. Cells were subsequently transfected with 1 nM of either *EFNB2* esiRNA or scrambled esiRNA for 72 h, after which *EFNB2* silencing was confirmed using RT-PCR using the same primers outlined in Table 1. Synaptophysin, Akt_T and Akt_{Pi} protein expression were assessed using quantitative western blotting. Neurite length and the number of neurites per cell were assessed using quantitative image analysis of five randomly chosen phase-contrast microscopic images as described above and expressed as average length

Table 1 Uses of primers and universal probes for the analysis of mRNA expression using real-time qPCR and RT-PCR

Gene name	GenBank accession number	Forward/reverse	Primer sequence	UPL number
EFNB2	NM_004093.2	Forward	5′-TCTTTGGAGGGCCTGGAT-3′	79
		Reverse	5′-CCAGCAGAACTTGCATCTTG-3′	
β-Actin	NM_001101.3	Forward	5′-CCAACCGCGAGAAGATGA-3′	64
		Reverse	5′-CCAGAGGCGTACAGGGATAG-3′	
GAPDH	NM_002046.3	Forward	5′-AGCCACATCGCTCAGACAC-3′	60
		Reverse	5′-GCCCAATACGACCAAATCC-3′	

Table 2 Uses of the primary and secondary antibodies for the detection of proteins using quantitative western blotting

Protein	Primary antibody	Secondary antibody
Recombinant NNMT	Mouse-anti-V5 (1 : 2000, Abcam, ab27671)	Goat-anti-mouse IgG (1 : 2000, Sigma, A4416)
Tyrosine hydroxylase	Rabbit-anti-tyrosine hydroxylase (1 : 200, Source Bioscience, GTX113016)	Goat-anti-rabbit IgG (1 : 2000, Sigma, A8275)
Tryptophan hydroxylase	Rabbit-anti-tryptophan hydroxylase (1 : 500, Source Bioscience, GTX109027)	Goat-anti-rabbit IgG (1 : 2000, Sigma)
Choline acetyltransferase	Rabbit-anti-choline acetyltransferase (1 : 500, Source Bioscience, GTX113163)	Goat-anti-rabbit IgG (1 : 2000, Sigma)
NeuN	Rabbit-anti-NeuN (1 : 100, Source Bioscience, GTX37604)	Goat-anti-rabbit IgG (1 : 2000, Sigma)
Ephrin B2	Mouse-anti-ephrin B2 (1 : 1000, Sigma, SAB4200120)	Goat-anti-mouse IgG (1 : 2000, Sigma)
Synaptophysin	Rabbit-anti-synaptophysin (1 : 500, Source Bioscience, GTX100865)	Goat-anti-rabbit IgG (1 : 2000, Sigma)
Akt	Rabbit-anti-Akt (1 : 500, Insight Biotechnology, 603401)	Goat-anti-rabbit IgG (1 : 2000, Sigma)
Phosho-Akt	Rabbit-anti-phospho-Akt (Ser473) (1 : 2000, New England Biolabs, 4060)	Goat-anti-rabbit IgG (1 : 5000, Sigma)
β-tubulin	Mouse-anti-β-tubulin (1 : 2000, Abcam, ab7792)	Goat-anti-mouse IgG (1 : 2000, Sigma)

All secondary antibodies were conjugated to horseradish peroxidase.

in μm ± S.E.M. The number of cells counted was 136 for scrambled esiRNA-treated and 135 for *EFNB2* esiRNA-treated cells.

Inhibition of Akt phosphorylation using LY294002. S.NNMT.LP cells were seeded at a density of 75 000 cells/ml and allowed to grow until approximately 75% confluent. Cells were incubated for 60 min in the presence or absence of 50 μM LY294002, after which the cells were lysed and Akt_T, Akt_{Pi} and synaptophysin expression were detected using western blotting.

Statistical analyses. All statistical analyses comprised comparison between SH-SY5Y and S.NNMT.LP using Student's *t*-test with Welch correction. The exception was the comparison of the effect of MeN upon SH-SY5Y morphology, which comprised one-way ANOVA with Tukey's *post hoc* comparisons. For all analyses, $P < 0.05$ was taken as significant.

Conflict of Interest

The authors declare no conflict of interest.

Acknowledgements. This work was supported by Parkinson's UK (grant number 0505).

1. Aksoy S, Szumlanski CL, Weinshilboum RM. Human liver nicotinamide *N*-methyltransferase. cDNA cloning, expression, and biochemical characterisation. *J Biol Chem* 1994; **269**: 14835–14840.
2. Parsons RB, Smith ML, Williams AC, Ramsden DB. Expression of nicotinamide *N*-methyltransferase (E.C. 2.1.1.1) in the Parkinsonian brain. *J Neurol Exp Neurol* 2002; **61**: 111–124.
3. Kassem HS, Sangar V, Cowan R, Clarke N, Margison GP. A potential role of heat shock proteins and nicotinamide *N*-methyltransferase in predicting response to radiation in bladder cancer. *Int J Cancer* 2002; **101**: 454–460.
4. Roessler M, Rollinger W, Palme S, Hagmann ML, Berndt P, Engel AM *et al.* Identification of nicotinamide *N*-methyltransferase as a novel serum tumour marker for colorectal cancer. *Clin Cancer Res* 2005; **11**: 6550–6557.
5. Tomida M, Ohtake H, Yokota T, Kobayashi Y, Kurosumi M. Stat3 up-regulates expression of nicotinamide *N*-methyltransferase in human cancer cells. *J Cancer Res Clin Oncol* 2008; **134**: 551–559.
6. Kim J, Hong SJ, Lim EK, Yu YS, Kim SW, Roh JH *et al.* Expression of nicotinamide *N*-methyltransferase in hepatocellular carcinoma is associated with poor prognosis. *J Exp Clin Cancer Res* 2009; **28**: 20.
7. Emanuelli M, Santarelli A, Sartini D, Ciavarella D, Rossi V, Pozzi V *et al.* Nicotinamide *N*-methyltransferase upregulation correlates with tumour differentiation in oral squamous cell carcinoma. *Histol Histopathol* 2010; **25**: 15–20.
8. Sternak M, Khomich TI, Jakubowski A, Szafarz M, Szczepański W, Białas M *et al.* Nicotinamide *N*-methyltransferase (NNMT) and 1-methylnicotinamide (MNA) in experimental hepatitis induced by concanavalin A in the mouse. *Pharmacol Rep* 2010; **62**: 483–493.
9. Kim HC, Mofarrahi M, Vassilakopoulos T, Maltais F, Sigala I, Debigare R *et al.* Expression and functional significance of nicotinamide *N*-methyltransferase in skeletal muscle of patients with chronic obstructive pulmonary disease. *Am J Respir Care Med* 2010; **181**: 797–805.
10. Parsons RB, Smith SW, Waring RH, Williams AC, Ramsden DB. High expression of nicotinamide *N*-methyltransferase in patients with idiopathic Parkinson's disease. *Neurosci Lett* 2003; **342**: 13–16.
11. Parsons RB, Aravindan S, Kadampeswaran A, Evans EA, Sandhu KK, Levy ER *et al.* The expression of nicotinamide *N*-methyltransferase increases ATP synthesis and protects SH-SY5Y human neuroblastoma cells against the toxicity of Complex I inhibitors. *Biochem J* 2011; **436**: 145–155.
12. Tang SW, Yang TC, Lin WC, Chang WH, Wang CC, Lai MK *et al.* Nicotinamide *N*-methyltransferase induces cellular invasion though activating matrix metalloproteinase-2 expression in clear renal cell carcinoma cells. *Carcinogenesis* 2011; **32**: 138–145.
13. Fredrich M, Illing RB. MMP-2 is involved in synaptic remodelling after cochlear lesion. *Neuroreport* 2010; **21**: 324–327.
14. Song G, Ouyang G, Bao S. The activation of Akt/PKB signalling pathway and cell survival. *J Cell Mol Med* 2005; **9**: 59–71.
15. Burke RE. Inhibition of mitogen-activated protein kinase and stimulation of Akt kinase signalling pathways: two approaches with therapeutic potential in the treatment of neurodegenerative disease. *Pharmacol Ther* 2007; **114**: 261–277.
16. Levy OA, Malagelada C, Greene LA. Cell death pathways in Parkinson's disease: proximal triggers, distal effectors and final steps. *Apoptosis* 2009; **14**: 478–500.
17. Namikawa K, Honma M, Abe K, Takeda M, Mansur K, Obata T *et al.* Akt/protein kinase B prevents injury-induced motor neuron death and accelerates neuronal regeneration. *J Neurosci* 2000; **20**: 2875–2886.
18. Du Y, Li X, Yang D, Zhang X, Chen S, Huang K *et al.* Multiple molecular pathways are involved in the neuroprotection of GDNF against proteasome inhibitor induced dopamine neuron degeneration *in vivo*. *Exp Biol Med (Maywood)* 2008; **233**: 881–890.

19. Timmons S, Coakley MF, Moloney AM, O'Niel C. Akt signal transduction dysfunction in Parkinson's disease. *Neurosci Lett* 2009; **467**: 30–35.
20. Cheung YT, Lau WK, Yu MS, Lai CS, Yeung SC, So KF *et al.* Effects of all-*trans*-retinoic acid on human SH-SY5Y neuroblastoma as *in vitro* model in neurotoxicity research. *Neurotoxicology* 2009; **30**: 127–135.
21. Malagelada C, Jin D, Greene LA. RTP-801 is induced in Parkinson's disease and mediates neuron death by inhibiting Akt phosphorylation/activation. *J Neurosci* 2008; **28**: 14363–14371.
22. Sagi Y, Mandel S, Amit T, Youdim MB. Activation of tyrosine kinase receptor signaling pathway by rasagiline facilitates neurorescue and restoration of nigrostriatal dopamine neurons in post-MPTP-induced parkinsonism. *Neurobiol Dis* 2007; **25**: 35–44.
23. Steinle JJ, Meininger CJ, Forough R, Wu G, Wu MH, Granger HJ. Eph B4 receptor signaling mediates endothelial cell migration and proliferation via the phosphatidylinositol 3-kinase pathway. *J Biol Chem* 2002; **277**: 43830–43835.
24. Feldmann G, Habbe N, Dhara S, Bisht S, Alvarez H, Fendrich V *et al.* Hedgehog inhibition prolongs survival in a genetically engineered mouse model of pancreatic cancer. *Gut* 2008; **57**: 1420–1430.
25. Georgakopoulos A, Xu J, Xu C, Mauger G, Barthet G, Robakis NK. Presenilin1/gamma-secretase promotes the EphB2-induced phosphorylation of ephrinB2 by regulating phosphoprotein associated with glycosphingolipid-enriched microdomains/Csk binding protein. *FASEB J* 2011; **25**: 3594–3604.
26. Dalva MB, Takasu MA, Lin MZ, Shamah SM, Hu L, Gale NW *et al.* EphB receptors interact with NMDA receptors and regulate excitatory synapse formation. *Cell* 2000; **103**: 945–956.
27. Henkemeyer M, Itkis OS, Ngo M, Hickmott PW, Ethell IM. Multiple EphB receptor tyrosine kinases shape dendritic spines in the hippocampus. *J Cell Biol* 2003; **163**: 1313–1326.
28. McClelland AC, Sheffler-Collins SI, Kayser MS, Dalva MB. Ephrin-B1 and ephrin-B2 mediate EphB-dependent presynaptic development via syntenin-1. *Proc Natl Acad Sci USA* 2009; **106**: 20487–20492.
29. Chen Y, Fu WY, Ip JP, Ye T, Fu AK, Chao MV *et al.* Ankyrin repeat-rich membrane spanning protein (kidins220) is required for neurotrophin and ephrin receptor-dependent dendrite development. *J Neurosci* 2012; **32**: 8263–8269.
30. Sloniowski S, Ethell IM. Looking forward to EphB signaling in synapses. *Semin Cell Dev Bio* 2012; **23**: 75–82.
31. Perović M, Mladenović A, Rakić L, Ruzdijić S, Kanazir S. Increase of GAP-43 in the rat cerebellum following unilateral striatal 6-OHDA lesion. *Synapse* 2005; **56**: 170–174.
32. Hayes L, Ralls S, Wang H, Ahn S. Duration of Shh signaling contributes to mDA neuron diversity. *Dev Biol* 2013; **374**: 115–126.
33. Ran X, Qin H, Liu J, Fan JS, Shi J, Song J. NMR structure and dynamics of human ephrin-B2 ectodomain: the functionally critical C-D and G-H loops are highly dynamic in solution. *Proteins* 2008; **72**: 1019–1029.
34. Yavrouian EJ, Sinha UK, Rice DH, Salam MT, Gill PS, Masood R. The significance of ephB4 and ephrinB2 expression and survival in head and neck squamous cell carcinoma. *Arch Otolaryngol Head Neck Surg* 2008; **134**: 985–991.
35. Ishii K, Oda Y, Ichikawa T, Deguchi T. Complementary DNAs for choline acetyltransferase from spinal cords of rat and mouse: nucleotide sequences, expression in mammalian cells, and *in situ* hybridization. *Brain Res Mol Brain Res* 1990; **7**: 151–159.
36. Oda Y, Nakanishi I, Deguchi T. A complementary DNA for human choline acetyltransferase induces two forms of enzyme with different molecular weights in cultured cells. *Brain Res Mol Brain Res* 1992; **16**: 287–294.
37. Kim KK, Adelstein RS, Kawamoto S. Identification of neuronal nuclei (NeuN) as Fox-3, a new member of the Fox-1 gene family of splicing factors. *J Biol Chem* 2009; **284**: 31052–31061.
38. Sarkanen JR, Nykky J, Siikanen J, Selinummi J, Ylikomi T, Jalonen TO. Cholesterol supports the retinoic acid-induced synaptic vesicle formation in differentiating human SH-SY5Y neuroblastoma cells. *J Neurochem* 2007; **102**: 1941–1952.
39. Xie HR, Hu LS, Li GY. SH-SY5Y human neuroblastoma cell-line: *in vitro* cell model of dopaminergic neurons in Parkinson's disease. *Chin Med J (Engl)* 2010; **123**: 1086–1092.
40. Encinas M, Iglesias M, Liu Y, Wang H, Muhaisen A, Ceña V *et al.* Sequential treatment of SH-SY5Y cells with retinoic acid and brain-derived neurotrophic factor gives rise to fully differentiated, neurotrophic factor-dependent, human neuron-like cells. *J Neurochem* 2000; **75**: 991–1003.
41. Agholme L, Lindström T, Kågedal K, Marcusson J, Hallbeck M. An *in vitro* model for neuroscience: differentiation of SH-SY5Y cells into cells with morphological and biochemical characteristics of mature neurons. *J Alzheimers Dis* 2010; **20**: 1069–1082.
42. Kanthasamy AG, Anantharam V, Zhang D, Latchoumycandane C, Jin H, Kaul S *et al.* A novel peptide inhibitor targeted to caspase-3 cleavage site of a proapoptotic kinase protein kinase C delta (PKCδ) protects against dopaminergic neuronal degeneration in Parkinson's disease models. *Free Radic Biol Med* 2006; **41**: 1578–1589.
43. Zhou W, Bercury K, Cummiskey J, Luong N, Lebtin J, Freed CR. Phenylbutyrate up-regulates the DJ-1 protein and protects neurones in cell culture and in animal models of Parkinson disease. *J Biol Chem* 2011; **286**: 14941–14951.
44. Adams FS, La Rosa FG, Kumar S, Edwards-Prasad J, Kentroti S, Vernadakis A *et al.* Characterisation and implantation of two neuronal cell-lines with dopaminergic properties. *Neurochem Res* 1996; **21**: 619–627.
45. Fukushima T, Tawara T, Isobe A, Hojo N, Shiwaku K, Yamane Y. Radical formation site of cerebral Complex I and Parkinson's disease. *J Neurosci Res* 1995; **42**: 385–390.
46. Fukushima T, Kaetsu A, Lim H, Moriyama M. Possible role of 1-methylnicotinamide in the pathogenesis of Parkinson's disease. *Exp Toxicol Pathol* 2002; **53**: 469–473.
47. Mori Y, Sugawara A, Tsuji M, Kakamu T, Tsuboi S, Kanda H *et al.* Toxic effects of nicotinamide methylation on mouse brain striatum neuronal cells and its relation to manganese. *Environ. Health Prev Med* 2012; **17**: 371–376.
48. Williams AC, Ramsden DB. Autotoxicity, methylation and a road to the prevention of Parkinson's disease. *J Clin Neurosci* 2005; **12**: 6–11.
49. Lam PM, Hainsworth AH, Smith GD, Owen DE, Davies J, Lambert DG. Activation of recombinant human TRPV1 receptors expressed in SH-SY5Y human neuroblastoma cells increases [Ca(2 +)](i), initiates neurotransmitter release and promotes delayed cell death. *J Neurochem* 2007; **102**: 801–811.
50. Jiang H, Jiang Q, Feng J. Parkin increases dopamine uptake by enhancing the cell surface expression of dopamine transporter. *J Biol Chem* 2004; **279**: 54380–54386.
51. Ault DT, Werling LL. SH-SY5Y cells as a model for sigma receptor regulation of potassium-stimulated dopamine release. *Brain Res* 2000; **877**: 354–360.

Supplementary Information accompanies this paper on Cell Death and Disease website (http://www.nature.com/cddis)